

ELECTRONIC SPECTROSCOPY OF OZONE. II. VISIBLE AND NEAR UV REGION

I.M. Sizova

*P.N. Lebedev Physics Institute,
Russian Academy of Sciences, Moscow*

Received March 19, 1993

This paper is the second part of the review summarizing experimental and theoretical data compiled till 1991 including the data on electronic structure and electronic absorption spectra of the ozone molecules in the region from near IR to the far UV. This part of the study presents information about the interaction of the ozone molecules with radiation in the visible (Chappuis bands) and near UV (Huggins bands) regions.

The first part of the overview concerning the electronic spectroscopy of ozone that presents general information about the electronic absorption spectra and structure of electronic energy levels of the ozone molecule, as well as detailed information about the ozone molecular characteristics in the energy region near the limit of its dissociation from the ground state has been earlier published in the journal "Atmospheric and Oceanic Optics" **6**, No. 5, 1993 and below it is referred to as Part 1. Since references in both parts of the overview overlap the list of references, in this part, it involves that from the Part 1 under their numbers in it and then it is completed with new ones.

Numbering of the spectral regions with Roman numerals that you will find in the below subtitles is taken from Fig. 2 of the Part 1 which presents the whole absorption spectrum of ozone starting with the dissociation limit at 1.05 eV and to the ionization continuum (up to 30 eV), as it has been obtained in Ref. 21 using the method of electron losses at small angles for the hitting electrons of 300 eV energy.

1. ABSORPTION SPECTRUM OF O₃ MOLECULE IN THE VISIBLE REGION. CHAPPUIS BAND AT 2–2.3 eV (REGION II)

1.1. Identification of an electronic transition.

Known diffusion absorption band of the ozone in the visible region (540–620 nm) discovered as early as 1882 (see Ref. 3) is, according to theoretical calculations, due to a weak dipole-allowed transition $X^1A_1 \rightarrow 1^1B_1$ (oscillator strength $f \approx (2-3) \cdot 10^{-5}$, see Table III, Part 1) and, possibly, due to the electron dipole-forbidden, but allowed taking into account the antisymmetric stretch, transition $X^1A_1 \rightarrow 1^1A_2$.

At present two mechanisms of interaction between the ozone molecule and light are assumed to work when interpreting the origin of Chappuis absorption band. According to the first scheme, which is based on a comparison of theoretically calculated and experimentally observed positions of the band and oscillator strengths of the transitions forming it, the main contribution to the absorption comes from the transition $X^1A_1 \rightarrow 1^1B_1$. At the same time one can see from Fig. 3 (Part 1) that minimum of the 1^1B_1 surface is essentially lower than that for the corresponding to its dissociation products

$O(^1D) + O_2(^1\Delta_g)$ and, as a consequence, strong interaction, owing to antisymmetric stretch of the 1^1B_1 state, between this state and the dissociative (or weakly bound) 1^1A_2 state correlating with the fragments $O(^3P) + O_2(^3\Sigma_g^-)$ described in Ref. 22 practically results in a predissociation of the ozone molecule due to absorption in Chappuis band what yields unexcited products as it is actually observed in the light absorption experiments^{50,85,87,91–96} and follows from the analysis of the dissociation products.^{97–100} It should be noted here that both these states are from the C_s symmetry class and have the same symmetry $^1A''$ and, hence, the interaction occurs due to repulsion in the region of intersection.

However, in Refs. 76 and 101 we find a different mechanism proposed for the interaction between light and the ozone molecule due to absorption in Chappuis band. According to this approach a molecule of ozone in the state X^1A_1 absorbs light and comes to a metastable (weakly bound) state 1^1A_2 , in which it lives at least 200 microseconds. From this state the molecule can either relax to a vibrationally excited ground state or dissociate yielding O and O₂ fragments. This can occur due to collisions, intersection with the ground electronic state, as well as due to fluorescence (of course taking into account Franck–Condon principle). Unfortunately, this mechanism was proposed based only on the results of indirect experiments. The authors observed a transient absorption spectrum in the UV region under conditions of the ozone photolysis due to absorption in Chappuis band and revealed that it is distinct from the transient spectrum of ozone molecules in a vibrationally excited ground state.^{102–104} Other reasons for proposing this interaction mechanism were the coincidence of the transient spectrum maximum (near 320 nm) with the energy of the dipole-allowed transition $1^1A_2 \rightarrow 2^1B_1$ (approximately 3.8 eV energy⁷) and the absence of dissociation during 200 microseconds though under the photolysis that occurs. Besides, the majority of theoretical calculations do not give a potential surface of the state 1^1A_2 related to the dissociation (see Fig. 3 in Part 1).

As a matter of fact the latter scheme of the interaction process due to absorption in Chappuis band does not contradict the former one since excitation of

1^1A_2 state can take place not directly from the X^1A_1 state but via 1^1B_1 state owing to the interaction between the surfaces 1^1B_1 and 1^1A_2 , as was mentioned above. Time characteristics of the absorption process, of the transition between the potential surfaces, and of the O_3 molecule decay and/or relaxation into the ground state are the factors that determine an actual path of the process. Therefore, the final decision on choosing the model can be done only based on additional investigations of time characteristics of the dissociation due to absorption in Chappuis band and of the fluorescence, as it was done for the case of Hartley absorption band in the UV. More accurate (compared to already achieved precision) determination of the quantum yield of the dissociation is also needed.

A little bit different point of view on the transition path has been recently presented in Refs. 50 and 66. It is based on the observations of two different structures in Chappuis absorption band. The authors of Ref. 66 have measured the ozone absorption spectrum not only in the gas phase but also in a solution of ozone in CCl_4 at room temperature, in its solution in liquid O_2 at 77 K, and in solid phase ozone (film).

From the analysis of the spectrum shift, its broadening, variation of the ratio of the absorption cross sections in different spectral regions, and taking into account small value of the oscillator strength ($f \approx 3.2 \cdot 10^{-5}$) the authors arrived at a conclusion that most probable explanation of Chappuis band origin is a simultaneous transition into two states that, by their energies, are close to degeneration. One of these states which determines the basic profile of the band is, in the authors opinion, the above mentioned state 1^1A_2 while another one being presumably either 1^3A_2 or 1^3B_2 . Such a transition scheme well agrees with the transformations of the absorption spectrum due to the solvents surroundings and with that observed in solid phase. However, analysis of the transformations is rather qualitative and therefore it can not be considered rigorous.

A quantitative grounding for the dual transition (or to say strictly of at least dual transition) model of Chappuis absorption band formation was obtained by Anderson and co-workers⁵⁰ from a comparative analysis of the absorption spectra of $^{16}O_3$ and $^{18}O_3$ ozone isotopes.

Earlier⁴⁹ the same group had similarly investigated Wulf absorption bands that border upon the long wave side of Chappuis band and determined the adiabatic energy of the 1^1A_2 surface assuming the Wulf bands to be due to the transition $X^1A_1 \rightarrow 1^1A_2$ (for more detail see Part 1). Now, in Ref. 50 they show that Chappuis band is due to a transition at least into two strongly overlapping electronic states. One of them, the upper state that determines the major portion of the observed spectrum, is 1^1B_1 state with the adiabatic energy of 16500 cm^{-1} (2.05 eV), which earlier has already been related to Chappuis band. Since angles of the states X^1A_1 and 1^1B_1 are close and because of a strong distinction in the bond lengths of these states (see Table II in Part 1) the structure of this transition is basically a simple progression in the mode ν_1 . According to Ref. 50 this progression is $X^1A_1(000) \rightarrow 1^1B_1(\nu'_1, \nu'_2 = 2.0)$ with $\omega'_1 \approx 1210 \text{ cm}^{-1}$ and $\omega'_2 \approx 640 \text{ cm}^{-1}$ and $\nu'_2 = 2$ in contrast to earlier (Wulf) assumed $\nu'_2 = 0$.

The second electronic state that contributes to Chappuis band formation has, according to Ref. 50, the adiabatic energy of 15750 cm^{-1} (1.95 eV) what is only 750 cm^{-1} lower than that of the state 1^1B_1 . This energy level is attributed in Ref. 50 to one of two triplet states: 2^3B_2 and 1^3B_1 . Presumably this state is 2^3B_2 . This state is responsible for the band near 17414 cm^{-1} and most likely for the specific features of the absorption spectrum in the condensed phase observed in Ref. 66.

Thus, the model by Anderson⁵⁰ is close to that proposed by Vaida and co-workers.⁶⁶ The main distinction between these models is that, according to the former one, the main portion of the spectrum is attributed to the transition $X^1A_1 \rightarrow 1^1B_1$ while in Ref. 66 the transition $X^1A_1 \rightarrow 1^1A_2$ is assumed to be responsible for it. Moreover, the authors of Ref. 50 do not exclude that 1^1A_2 state also plays a certain role in the formation of Chappuis absorption band. They do so first of all because the Wulf bands⁶⁶ ($X^1A_1 \rightarrow 1^1A_2$) that border upon the red side of Chappuis band partially disturb its wing and, second, because the products, $O + O_2$, produced as a result of light absorption in Chappuis band, are in the ground states (see below for more detail). The state 1^1A_2 correlates with these states of the fragments and is a dissociative state of the ozone molecule while the state 1^1B_1 correlates with the states of excited products $O(^1D) + O_2(^1\Delta_g)$ and it is a bound state. This means that at some moment after the absorption of a light quantum (or during this process) there must occur an internal transition from 1^1B_1 state to the state of the products $O + O_2$, possibly into 1^1A_2 state.

The latter fact is partially analogous to the situation with Hartley band though there are two essential distinctions between them. Therefore it should be thoroughly investigated. The first distinction is in the fact that absorption of light in Hartley band can result in the molecule dissociation through two dissociation channels (for more detail see the below Sections of this overview) while in the case of absorption within Chappuis band only one channel works and, moreover, it should yield only unexcited dissociation products. The second distinction is as follows. The authors of Ref. 50 carried out the Fourier spectral analysis of Chappuis band similar to that undertaken in order to elucidate the origin of small peaks in Hartley absorption band. Such an analysis showed that Chappuis band has much simpler and more distinct structure than Hartley band what is indicative of much simpler structure of the upper surfaces of the transition forming it. It is especially interesting, in this connection, to make analysis of both these bands in parallel using similar techniques. As a matter of fact, such a work is being done, for example by Valentini and his co-workers, when studying the photolysis products (see below).

In a recent paper by Banichevich¹³⁶ it was proposed one more and better grounded version of a dual transition model of Chappuis band formation. In contrast to models from Refs. 50 and 66 this one does not involve triplet states while uniting two basic single transition models, that means it assumes the formation of Chappuis band to be due to simultaneous transition into 1^1A_2 and 1^1B_1 states. When making *ab initio* calculations^{41,136} of the potential surfaces of 1^1A_2 and 1^1B_1 states in C_{2v} and C_s symmetries the authors confirmed (as it was shown in

Ref. 22) that in the dissociation geometry C_s the states 1^1A_2 and 1^1B_1 , being the states of the same symmetry class $1^1A''$, intersect and repel thus forming the states C^1A'' and D^1A'' . Transitions into both these states from X^1A_2 state are dipole-allowed since they are linear combinations of 1^1A_2 and 1^1B_1 states. Under vertical excitation 1^1B_1 state is lower than 1^1A_2 (2.10 and 2.16 eV energies, respectively) while positions of their potential minima, also belonging to the symmetry class C_{2v} , are in the opposite order (1.82 and 1.44 eV). The intersection of 1^1A_2 and 1^1B_1 states occurs just in the Franck-Condon region (F-C). The lower of thus formed states, C^1A'' , is a repulsive state in the F-C region, it correlates with unexcited dissociation products and reaches its minimum out of the F-C region near the bending angle $\vartheta = 100^\circ$. Just this state determines the main features of Chappuis band profile and states of the photodissociation products. The second state, D^1A'' , is a bound state in the F-C region (geometry of its minimum is close to that of X^1A_1 state). This state correlates with the excited products. Transition to this state determines the vibrational structure in the short-wave portion of the band. Moreover, because of noticeable instability in the dipole moments of the transitions $X^1A_1 \rightarrow C^1A''$ and $X \rightarrow D$ (also calculated *ab initio* in Ref. 136) the maximum of the band has two peaks corresponding to the transitions to states $v_1' = 2$ and 3 while the transitions to states $v_1' = 1$ and 2 contribute to the long-wave portion of the band though not distinctly visible against the background of the main band profile because of their low

intensity. By taking one-dimensional section of the potential surfaces of C^1A'' and D^1A'' states in the C_s symmetry the authors of Ref. 136 have calculated Chappuis band assuming that light absorption in C and D states occurs independently. As a result, they managed to reconstruct all peculiarities of the band very well. The remaining disagreements (mainly, general shift and difference in the widths of the basic band profile) are most likely due to a displacement of the potential surfaces relative to zero, inaccurate setting of their slopes in the F-C region, as well as due to certain simplifications used (ignorance of the temperature finiteness, interaction between C and D states, the vibrations and rotations bonding, 3-D character of motion, etc). In addition, it is shown in Ref. 136 that the longer wave Wulf bands usually assigned to the transition $X^1A_1 \rightarrow 1^1A_2$ (see Part 1) and temperature dependences of their intensities are quite well described within the frameworks of the transition $X^1A_1 \rightarrow C^1A''$ near its minimum. Further validation of this model needs for a thorough experimental studies of the states of dissociation fragments produced due to absorption in Chappuis band and for measurements of absorption in the region between Chappuis and Huggins bands (see below). Calculations of three dimensional cross sections are also desirable.

1.2. Absorption cross sections. Detailed experimental studies of the ozone absorption spectrum in Chappuis band were being permanently carried out during last 50 years. Basic results of these studies are shown in Fig. 1 and listed in Table I, which summarizes all experimental data on the ozone absorption cross sections in the UV and visible regions.

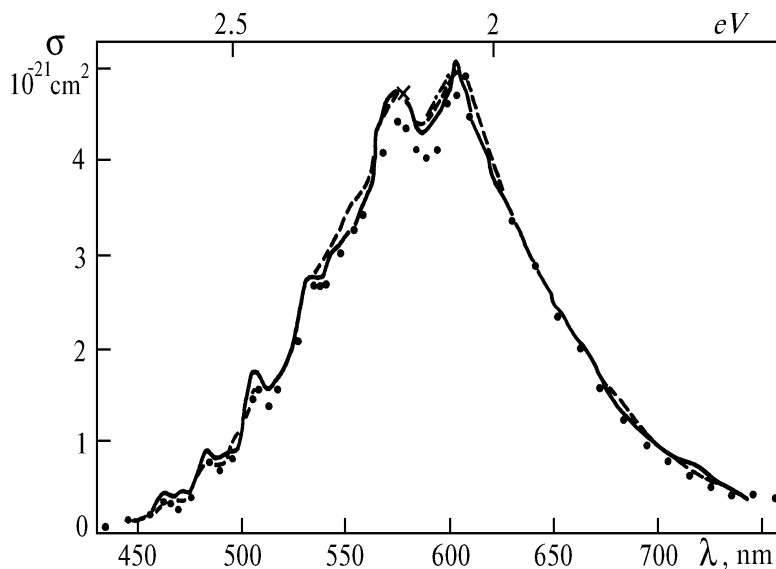


FIG. 1. The absorption spectrum in Chappuis band at room temperature: 300 K, 1953 (Ref. 87 and 91) (dots); 291 K, 1952/53 (Ref. 92 and 93) (solid line); 294 K, 1961 (Ref. 94) (crosses); 303 K, 1968 (Ref. 85) (dashed line); and, 230 and 299 K, 1990 (Ref. 96) (dashed-dotted line).

TABLE I..

Authors, year, references, remarks	Light source	Spectral region λ , nm	Spectral resolution $\pm \Delta\lambda$, nm	T , K	Error in cross section value, %
1	2	3	4	5	6
Vigroux, 1952–1953, Refs. 92 and 93 Only qualitative view of the spectrum and extrema positions are presented at $\lambda = 365\text{--}385$ nm	lamp: continuous spectrum + separate lines	230 – 245 245 – 313 313 – 340 340 – 346 346 – 365 365 – 385 407 – 483 483 – 530 530 – 650 650 – 740		291 181; 198; 214 229; 243; 291 181; 198; 214 229; 243; 291 323; 358; 393 291; 323; 358 393 291 291 291 181; 291 181; 291; 323 358; 393 291	
Inn, Tanaka, 1953, Refs. 87 and 91	lamp: continuous spectrum	200 – 352 434 – 756	1 1	300 300	5 5
Tanaka, Inn, Watanabe 1953–1956, Refs. 88 and 105 Only plots of cross sections are presented		105 – 220		~ 298	10
Ogawa, Cook, 1958, Ref. 106	lamp: discrete spectrum	52 – 135		~ 298	< 20
Hearn, 1961, Ref. 94	mercury lines	253.65 289.36 296.73 302.15 334.15 576.96	≈ 0.09 ≤ 0.01 ≤ 0.01 ≤ 0.01 ≤ 0.01 ≤ 0.01	295 292 295 293 293 294	≈ 2.5 ≈ 2.5 ≈ 2.5 ≈ 2.5 ≈ 2.5 ≈ 2.5
Jones, Davidson, 1962, Ref. 107 Only plots of relative cross sections are presented except for $T = 298$ K		248.5 297.5		300–900 300–900	~ 2 ~ 2
DeMore, Raper, 1964, Ref. 108	lamp: continuous spectrum	200 – 310	0.2	77.4–liquid nitrogen; 87.5–liquid Ar; 81.5–liquid CO; ~ 300	4
Griggs, 1968, Ref. 85 Only the figures of cross sections are presented	lamp: continuous spectrum	200 – 850	UV – 0.2 nm; visible – 1.5 nm	~ 303	≤ 1.5 for 200–300 nm; up to 6 for $\lambda > 300$ nm
Simons, Paur, Webster, 1973, Ref. 109 Only plots of cross sections at $T = 300$ and 195 K are presented		200 – 370		195; 300; 333	
Celotta, Mielczarek, Kuyatt, 1974, Ref. 21 Only plots of cross sections are presented	Spectrum of losses of high energy electrons at scattering at small angles (dipole–allowed transitions)	40 – 1244	~ 0.035 eV	~ 298	
Swanson, Celotta, 1975, Ref. 68 Only plots of cross sections are presented	Spectrum of losses of electrons with near threshold energies at scattering at large angles (dipole–forbidden transitions)	550 – 950		~ 298	
Moortgat, Warneck, 1975, Ref. 110	xenon lamp: continuous spectrum	297.5 – 330	0.3	298	

TABLE I continued.

1	2	3	4	5	6
Hanvey, McGrath, 1975, Ref. 111 Only plots of cross sections are presented relative to those at $T = 298$ K	quartz-iodine lamp	220; 230 240; 270 290; 300		295 – 373	
Arnold, Comes, Moortgat, 1977, Ref. 112	hydrogen and mercury lamps	295 – 320	0.05	298	≤ 1
Fairchild, Lee, 1978, Ref. 113		250 – 300			
Katayama, 1979, Ref. 46 Analysis of the spectrum structure and isotopic effect for $^{16}\text{O}_3$ and $^{18}\text{O}_3$; only plots of separate regions are presented	hydrogen lamp, calibration on mercury lines	310 – 360	$\leq 7\text{cm}^{-1}$ cold bands $\leq 10\text{cm}^{-1}$ hot bands	~ 298 ; 196 dry ice	
McDade, McGrath, 1980, Ref. 103 Only plots of cross sections are presented	xenon lamp	250 – 350	2	293	
Bass, Paur, 1981, Ref. 95 Calibration by cross section at $\lambda = 254$ nm from Ref. 94		200 – 700	0.025	200 – 300	≤ 2
Astholz, Croce, Troe, 1982, Ref. 114 Data at $T=300, 500, 720,$ and 900 K are presented	xenon lamp	210 – 325	3	300 – 1050	
Freeman, Yoshino, Esmond, Parkinson, 1984, Ref. 115 Data on a magnetic tape; only cross sections at 323–327 nm and four of mercury lines: 289, 297, 302, and 334 nm are presented	xenon lamp: continuous spectrum	240 – 350	0.003	195	~ 1
Bass, Paur, 1981–1984, Ref. 117 Calibration on cross sections at $\lambda = 254$ nm from Ref. 94		245 – 350 through 0.05 nm	0.025	200 – 300	
Brion, Daumont, Malicet, 1983–1985, Refs. 118–120	continuous spectrum + mercury lines	253.65 289.36 296.73 302.15 334.15 310 – 350	~ 0.012 ~ 0.012 ~ 0.012 ~ 0.012 ~ 0.012 ~ 0.012	298 298 298 298 298 223; 294	310 – 325 nm: 2 325 – 340 nm: 4 340 – 350 nm: 6
Brion, Daumont, Malicet, Marche, 1985, Ref. 121 Comparative analysis of all of the literature data for mercury lines	five mercury lines	253.65 289.36 296.73 302.15 334.15		298 298 298 298 298	
Mauersberger, Barnes, Hanson, Morton, 1986–1987, Refs. 122–123	mercury line	253.65		297.5	0.7
Molina, Molina, 1986, Ref. 125 Only average data at $T=226$ and 298 K in every 0.5 nm are presented	deuterium lamp: continuous spectrum + mercury lines	185 – 350 in every 0.002 nm	0.07	226 – 298	≤ 1
Barnes, Mauersberger, 1987, Ref. 124	mercury lines	253.65		195 – 351	0.7
Yoshino, Freeman, Esmond, Parkinson, 1988, Ref. 116	13 mercury lines	238 – 335	0.001	195; 228; 295	0.7

TABLE I continued.

1	2	3	4	5	6
Cacciani, di Sarra, Fiocco, Amoruso, 1989, Ref. 126 Cross sections only at $T=220$ and 293 K are presented	xenon lamp: continuous spectrum + mercury lines	339 – 355	0.0012	220–293	3 – 4
Amoruso, Cacciani, di Sarra, Fiocco, 1990, Ref. 96 The values of slipping average on 0.5 nm	xenon lamp	590 – 610	0.05	230; 299	2
Anderson, Maeder, Mauersberger, 1991, Ref. 50 Analysis of structure and isotopic effect for $^{16}\text{O}_3$ and $^{18}\text{O}_3$; only plots are presented		450 – 830	0.5	298	

At the same time we can state that temperature dependence of the absorption cross section, which is informative about the absorption process dynamics and about the photodissociation process is much less studied. Quite short overview of this topic can be found in Ref. 96. Data on the temperature dependence (mostly obtained 40 to 50 years ago) are very inconsistent. According to these data the cross section increases as the temperature decreases. In the early studies (in 1940s, see bibliography in Ref. 96) such an increase was estimated as 10 to 20%, though in later works it was considered to be 1 to 3% (this value is confirmed in nowadays studies also) what is within the measurement errors. Thus, in papers by Vigroux^{92,93} it was shown that the temperature effect does not exceed $\pm 2\%$ in the temperature range from 181 to 353 K. In a recent paper by Amoruso and co-workers⁹⁶ they paid special attention to studies of the temperature dependence though in a narrow wavelength interval within Chappuis band (590–610 nm). At the measurement accuracy of 2% they obtained 1% growth of the absorption cross section when changing temperature from 299 to 230 K. Based on the statistical analysis of their data they are inclined to believe that the temperature change causes the shift of the band (approximately 0.13 nm towards shorter wavelength) rather than the cross section growth. No dependence of the spectrum on pressure has been observed experimentally (see Sec. 1 of Part 1). As to the other investigations concerning the absorption of light by ozone within Chappuis band, studies of Raman spectra should be mentioned first of all (see the overview in Ref. 63).

1.3. Analysis of the photolysis products. No dissociation products in electronic excited states have been observed so far in studies of the dissociation due to absorption within Chappuis band though possible energetically (through the spin-forbidden channel, see Table I in Part 1). Normally the probability of dissociation into unexcited products is estimated to be unity, accurate to several per cent.^{97,99,100,127}

As can be understood from Fig. 3, Part 1, a complicated structure of intersecting potential surfaces of different symmetries corresponding to different channels of dissociation should result in a nonthermal distribution of the energy states of the dissociation products for any of the above mechanisms of the ozone molecules excitation due to absorption in Chappuis band. The distribution of energy states of these products depends on the energy of a light quantum absorbed by the ozone molecule. Experimental data on the energy states of photofragments

produced due to absorption of light in Chappuis band available at present (see Table II) well confirm this fact. We used the following abbreviations for the measurement techniques in this table: ChI is for the technique of recording the fragments based on chemical ionization and transit time measurements in combination with rotation of the radiation polarization; cCARS is for a collisionless CARS spectroscopy of O_2 . Distribution of atomic oxygen over translational energy was obtained⁹⁷ assuming that $E_{\text{O}} = 2E_{\text{O}_2}$.

Analysis of photodissociation products yielding information about structure of potential surfaces and dynamics of a monomolecular decay can be found in papers by J.J. Valentini from Los Alamos^{98–100} (see Table II). These investigations have been carried out using CARS laser spectroscopy of the distribution of unexcited molecular oxygen $\text{O}_2(^3\Sigma_g^-)$ produced due to O_3 dissociation at absorption of light at 532 and 578 ± 2 nm over vibrational–rotational states.^{98,99} Similar studies have been undertaken in Ref. 100 but using much narrower nine laser wavelengths from the region 560–638 nm. The experimental conditions were chosen so that the dissociation of ozone molecule and formation of the CARS spectra took place in a collisionless regime, that means that $\Delta\tau_{\text{las}}, \Delta\tau_{\text{Diss.Prob.}} \ll \tau_{\text{Coll}}$. In order to reveal dependence of the above-mentioned distributions on the wavelength of incident radiation, each of two laser pulses used for CARS spectroscopy was alternatively delayed by 4 ns relative to the other one, so that dissociation of O_3 took place due to absorption of only one beam while providing intersection of the beams in time to yield the CARS spectra ($\Delta\tau_{\text{las}} \cong 6$ ns). These experiments allowed the following peculiarities of the decay process to be revealed:

- no oxygen molecules in the states with $\nu_{\text{vibr}} > 4$ are observed, though for $\lambda < 560$ nm the states with $\nu = 6$ or 7 are possible;
- a weak inversion of populations of the levels with $\nu = 2$ and 3 is observed;
- the distribution over rotational states for each ν level is about three to four times narrower than that described by the Boltzmann law at the same value of J_{max} ;
- J_{max} values are too large and grow with the decreasing λ and ν ;
- quite a large fraction of energy is released into the translational degrees of freedom of fragments.

TABLE II.

λ , nm	Radiation source	Measurement technique	$O_2(^3\Sigma_g^-)$		Translational energy E	Authors, year, reference
			Vibrational state ν	Rotational states J		
600	dye-laser Chromatix CMX - 4	ChI	0 : 1 : 2 \approx 64 : 26 : 10		$E_0 \geq 0.3$ eV at angle distribution $f(\theta) \approx 0.25 + \sin^2 \theta$	Fairchild et al. 1978, Ref. 97
532	second harmonic of Nd ³⁺ YAG: laser	cICASLs	18%; $\nu = 0 - 4$; inversion $\nu = 2$ and 3	16%; $J_{\max} \approx 31 - 37$	66%	Valentini et al. 1981/83, Refs. 98 and 99
578 \pm 2	tunable dye-laser	cICASLs	17%; $\nu = 0 - 4$; inversion $\nu = 2$ and 3	18%; $J_{\max} \approx 31 - 37$	65%	Valentini et al. 1981/83, Refs. 98 and 99
532 + 578 \pm 2	second harmonic of Nd ³⁺ YAG: laser + dye-laser	cICASLs	18%; $\nu = 0 - 4$; inversion $\nu = 2$ and 3	15%; $J_{\max} \approx 31 - 37$	67%	Valentini et al. 1981/83, Refs. 98 and 99
nine lines: 560;572;591; 596;599;606; 609;625;638	dye-laser Rhodamine 6G 610 and 590; pumping by the second harmonic of Nd ³⁺ YAG: laser	cICASLs	$\sim 10\%$ does not depend on λ ; weak inversion $\nu = 2$ and 3	$\sim 24\%$ only odd $J \geq 19$; big J_{\max} decreasing with increasing of λ and ν ; $\Delta J \approx \Delta J_{\text{room}} \approx$ $\approx (0.25 - 0.3)$ ΔJ_{Bolt} at J_{\max}	$\sim 66\%$; sharp and "hot" distribution	Levene et al. 1987, Ref. 100

Theoretical analysis of the experimental results⁹⁸⁻¹⁰⁰ has shown that Franck-Condon effects play a decisive role in formation of the distribution of dissociation products over vibrational states. Thus revealed vibrational distributions that occurred to be the same for all wavelengths of incident radiation, from 532 to 638 nm, except for $\lambda = 578$ nm, (though the change of energy released from the dissociation products achieved about 40%) well agree with the simple model of a vibrational adiabatic transition. Sharp distinction of the vibrational distribution of the dissociation products produced due to the absorption of radiation^{98,99} at $\lambda = 578$ nm (population of levels with $\nu = 1$ is two times higher while that of levels with $\nu = 2$ is four times lower than the population observed at absorption at other wavelengths) is not explained by the authors even in their paper¹⁰⁰ published later and they believe that this situation occurs due to an unclear mistake. As to the rotational distribution observed, it is well described within the framework of the so-called "modified impulsive rotational model"¹²⁸ they have developed and which accounts for contributions coming from initial rotation, bending vibration of O_3 molecule, vector correlation between rotations, and from bending and decay processes, provided all conservation laws are fulfilled. Such a scheme of vibrational adiabatic and rotational impulsive model of interaction bears certain information about the shape and structure of potential surfaces of low and upper energy states. Quite similar situation we have when analyzing Hartley absorption band. It is worth noting that vibrational-rotational distributions of $O_2(^3\Sigma_g^-)$ and $O_2(^1\Delta_g)$ produced due to absorption in Chappuis and Hartley bands, respectively, are, in fact the same, described by one and the same theoretical model. This means, in turn, that in both cases we will have similar structures of electronic

transitions as well as interactions between the upper intersecting potential surfaces. These peculiarities of the surfaces we shall discuss below in connection with analogous experiments by Valentini and co-workers carried out in Hartley absorption band.^{129,130}

1.4. Conclusions. Thus, the origin of Chappuis absorption band is related to a dipole-allowed transition from the ground electronic state X^1A_1 to a bound one, 1^1B_1 (correlating with the dissociation products $O(^1D) + O_2(^1\Delta_g)$) and/or to an electronic and dipole-forbidden but allowed taking into account antisymmetric stretching transition to a dissociation or weakly bound state, 1^1A_2 , that correlates with $O(^3P) + O_2(^3\Sigma_g^-)$ dissociation products. Strong interaction between 1^1B_1 and 1^1A_2 states of the C_s symmetry results in the predissociation of the ozone molecule into unexcited products (quantum yield is about 1) and in a nonequilibrium distribution of the energy of these products over translational degrees of freedom that depends on energy of the light quantum absorbed. Recent investigations definitely show that Chappuis absorption band is determined by two qualitatively different structures, the band itself being due to transition into, at least, two overlapping electronic states. Possibly, some contribution to the formation of Chappuis band vibrational structure comes from interaction with triplet states 1^3A_2 , 1^3B_2 , 2^3B_2 , and 1^3B_1 which have close energies. The absorption cross section within Chappuis band is less than 10^{-20} cm² and, accurate to 1-2 per cent, is independent of temperature within the range from 180 to 350 K. Within the pressure range below 1 atm the absorption cross section does not also depend on pressure what is confirmed, for example, by the spectrum recorded in Ref. 66 at much lower pressures.

2. ENERGY RANGE BETWEEN VISIBLE AND UV SPECTRA, 2.26 – 3.12 eV (REGION III)

According to the scheme presented in Fig. 3 (Part 1) the ozone molecule has no electronic states in the energy interval from 2.26 (edge of Chappuis band) to 3.12 eV

(edge of Huggins band) except for the triplet dissociative state, 2^3B_2 , transitions to which are forbidden. Therefore, the absorption spectrum in this region is formed by wings of nearby absorption bands and is characterized by very low absorption cross section (below 10^{-23} cm² in its middle).

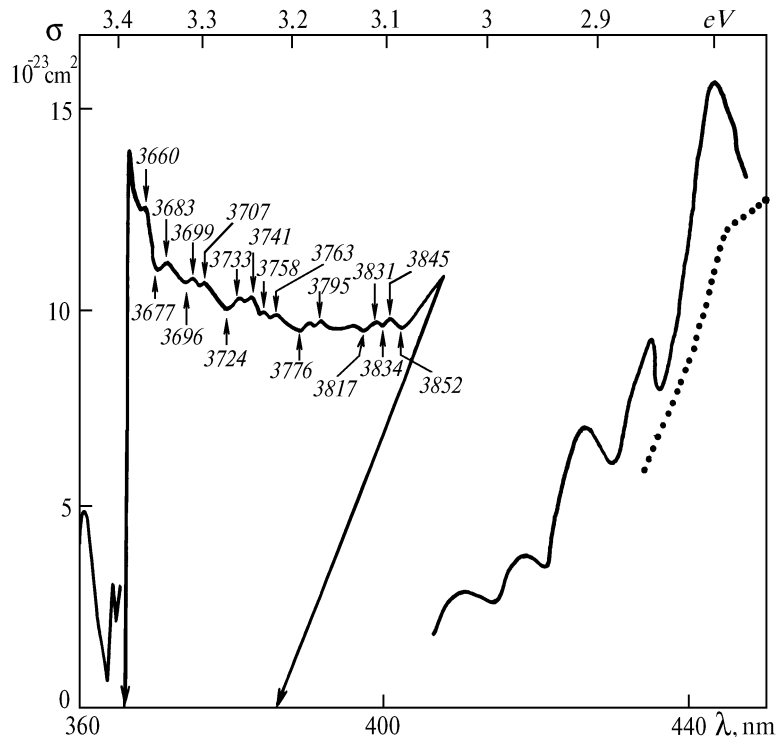


FIG. 2. Ozone absorption spectrum in the region of 360–450 nm (2.7–3.5 eV) at room temperature: 291 K, 1952/53 (Ref. 92–93) (solid line); 300 K, 1959 (Ref. 91) (dots). The portion of the spectrum from 366 and 386 nm was obtained in Refs. 92–93 only qualitatively. This spectrum is reproduced in the upper left part of the figure with maxima (at the top, in Å) and minima (at the bottom, in Å) positions indicated.

There are only few measurements available in literature for this region (see Fig. 2), all of them done about 40 years ago. No investigations of temperature dependence of the spectrum have been conducted. Only qualitative view of the spectrum in the region from 370 to 405 nm has been obtained in Refs. 92 and 93 and only order of magnitude estimations of the absorption cross section have been done. Structure of the spectrum in this range is evidently explained by the vibrational resonances in the nearby electronic states with a participation of high vibrational levels of the low or upper terms. On the short-wave edge the spectrum is strongly cut and in many features it is similar to the nearby Huggins bands. On the long-wave side the spectrum is more smooth like Chappuis band bordering upon it. It is a common rule, in atmospheric optics, to assume that ozone does not absorb light in this wavelength region what is justifiable for many practical applications.

3. NEAR UV SPECTRUM. HUGGINS BANDS, 3.12 – 4.0 eV (REGION IV)

Huggins absorption bands of ozone (310–390 nm) discovered⁴ in 1890 still attract much attention of researchers since they play an important role in atmospheric optics and because their short-wave boundary is within much stronger Hartley absorption band that makes the ozone gas the main absorber of harmful UV radiation from

the Sun. The boundary of these bands overlapping coincides with the limit of O dissociation into O(1D) and O₂($^1\Delta_g$) fragments. As known this reaction is the main source of chemically active excited atomic oxygen in the atmosphere. For these reasons identification of Huggins absorption bands is of certain practical interest. Besides, Huggins absorption bands are interesting themselves as an object for studying dynamics of photodissociation of small polyatomic molecules because they are diffuse bands due to predissociation and have a distinct vibrational structure.

3.1. Identification of the electronic transition.

Huggins absorption bands have a distinct vibrational structure with a weak continuum component characterized by very low absorption cross section. The bands extend from 310 nm at the short-wave edge, where they border upon much stronger though structureless Hartley band, to approximately 385 nm where there are hot lines of the bands.

Starting with the investigations by Yakovleva and Kondrat'jev¹³¹ in 1930s there were many attempts undertaken to identify the electronic transition responsible for this spectrum as well as for vibrational bands in it (see, for example, Refs. 7, 22, 45, 48, 71, 72, 90, 109, and 134).

For a long time it was believed, based on the analysis of the transition symmetry,^{7,22,71,72,90,109} that Huggins bands appear in the spectrum due to the same dipole-allowed transition, $X^1A_1 \rightarrow 1^1B_2$, as the adjacent Hartley absorption

band (this is not completely excluded till now, see Refs. 48, 132, 137, and 138). Strong differences in the structure and intensity of these bands are explained by the fact that Hartley band corresponds to the vertical fraction of the transition onto the upper vibrational levels of the state 1^1B_2 (oscillator strength $f \approx 10^{-1}$ (see Table III, Part 1) while Huggins bands are made up of nonvertical portion of the transition onto the low vibrational levels of the same state, 1^1B_2 , bound relative to the dissociation ($f \approx 10^{-4}$) in out of Franck–Condon region. A portion of the spectrum within Huggins bands (near 340 nm, or 3.65 eV, the so-called Chalonge–Lefebvre¹³³ band) was assigned⁷¹ to a very weak two–electron dipole–forbidden transition, $X^1A_1 \rightarrow 2^1A_1$, that causes certain modification of the bands in the region near 340 nm.

In Ref. 45 one can find a detailed analysis of Huggins absorption bands based on experimental data from Ref. 109. Analysis of the intensity of the bands and the transitions symmetry (activity of the v_3 odd parity states forbidden in the C_{2v} symmetry, according to Franck–Condon principle) allowed the authors of Ref. 45 to exclude the transitions to 1^1A_2 , 1^1B_2 , and 1^1B_1 states from the scheme and to identify all the observed bands as produced due to the transitions of the type $X^1A_1 \rightarrow 2^1A_1$. Since, according to theoretical calculations, the state 3^1A_1 lies about 3 to 4 eV higher than the region under consideration, being, in addition, dipole–allowed for transition from the ground state the state 2^1A_1 (6π) (see Fig. 3 in Part 1) remains to be the only candidate that correlates, in diabatic approximation, with the ring–shaped ozone molecule. Moreover, data on the equilibrium geometry of the upper state of Huggins transition obtained yet in Ref. 90 ($R = 1.383 \text{ \AA}$ and $\vartheta = 90^\circ 36'$) better correspond to the state 2^1A_1 than to the 1^1B_2 state (see Table II in Part 1).

The transition $X^1A_1(4\pi) \rightarrow 2^1A_1(6\pi)$ is the two–electron, dipole–forbidden transition what explains low intensity of Huggins absorption bands. One should take into account here that the state 2^1A_1 interacts (especially in the region where it borders upon Hartley band) with the state 1^1B_2 , ground state X^1A_1 , and with, at least, one repulsive state, R , that provides for ozone dissociation into unexcited products⁸³ (as is seen from Fig. 3, Part 1, both 1^1B_2 and 2^1A_1 states correlate with the excited dissociation products $O(^1D) + O_2(^1\Delta_g)$). A rough scheme of such an interaction is presented in Fig. 1 *b*, Part 1. A more thorough description of it will be presented below in the analysis of the transition making Hartley absorption band.

The calculations made in Ref. 45 showed that Huggins absorption bands have no continuum component, at least in the region out of the close vicinity of the limit at 310 nm, where they are perturbed by the Hartley band. It was also shown in these calculations that the rotational width of absorption lines, at temperature of 195 K, that could provide experimentally observed widths of the bands of 70 cm^{-1} must be $25 \pm 2 \text{ cm}^{-1}$. Note that rotational structure of the bands is unresolved in the spectrum because of diffuse character. The values R and ϑ for the equilibrium geometry of the state 2^1A_1 presented in Tables II and III of Part 1 (see also Fig. 3 in Part 1) as well as the oscillator strength, f , of the transition have been obtained from the calculations of spectrum using Franck–Condon principle and harmonic oscillator approximation. The above–mentioned band width of about 70 cm^{-1} and the rotational widths of spectral lines

of $25 \pm 2 \text{ cm}^{-1}$ correspond to the lifetime of vibrational level of the upper electronic state of $(1 - 2) \cdot 10^{-13} \text{ s}$, i.e., on the order of duration of several oscillations ($\tau_{\text{osc}} \approx (3 - 6) \cdot 10^{-14} \text{ s}$), what is in good agreement with the scheme of interaction between the bound state 2^1A_1 and a repulsive state R in the region near the short–wave boundary of Huggins band (see Fig. 1 in Part 1).

However, the interpretation of Huggins bands given by Brand⁴⁵ contradicts the experimental data obtained by Sinha⁴⁸ using a laser fluorescence spectroscopic technique to study spectra of a gas expanding in supersonic flow where the ozone was cooled so that it was possible to partially resolve the rotational structure of the spectrum ($T_{\text{rot}} \approx 3 \text{ K}$). Authors of this study dealt with two absorption bands in the region at 325 nm and came to a conclusion that these bands are due to transitions to the states (501) and (600), following the classification proposed in Ref. 46, that agree rather with the symmetry C_s for the upper state than with the C_{2v} symmetry. This, in turn, better agrees with the transition $X^1A_1 \rightarrow 1^1B_2$, nonvertical transition into the weakly bound (about 0.6 eV) portion of the potential surface of the state 1^1B_2 . That means that again, as in early studies, Huggins absorption bands are related to the same transition as Hartley band. This is also confirmed in a theoretical study carried out in Ref. 63 using Franck–Condon analysis in the Adler–Golden symmetry C_s . Moreover, in Ref. 48 the authors managed to estimate a predissociation lifetime of the state 1^1B_2 and it occurred to be about 3.6 fs what agrees with the estimate obtained from resonance Raman scattering spectra excited in Hartley absorption band. In addition, moments of inertia of the molecule in 1^1B_2 state have also been determined ($A = (2.1 \pm 0.4) \text{ cm}^{-1}$, $\bar{B} = (0.45 \pm 0.01) \text{ cm}^{-1}$) in this paper.

It should be noted here that interpretation of the spectra observed in Ref. 48 is mainly based on the assumption that identification of the absorption bands (of (501) band, in particular) carried out in Ref. 46 is wrong and this band should be identified as (502) band. However, Katayama, the author of Ref. 46, disagreed with this assumption and in his new paper¹³⁴ he presented a revised analysis of those data. Based on the study of isotopic shift of the band (501) he has arrived at a conclusion that by no reasons this band can be interpreted as (502) band. Thus, it is obvious that at present the question on the exact identification of the upper state of the transition yielding Huggins absorption band is still open.

Some serious arguments more that favor the identification of Huggins bands as the transition $X^1A_1 \rightarrow 1^1B_2$ have been recently presented by Le Quere and Leforestier.^{137,138} The failures of the earlier attempts to describe these bands according to this scheme they referred, and quite reasonably, to a poor quality of the potential surface of the 1^1B_2 state from Ref. 15 traditionally used for such calculations. In Refs. 137 and 138 the authors present new *ab initio* calculations of the potential surfaces of X^1A_1 , 1^1B_2 , and 2^1A_1 states, which, as in Ref. 15, are reduced to the standards of presentation in terms of analytical Sorby–Murel functions. Thus obtained potential surface of the 1^1B_2 state has a number of advantages compared to that in Ref. 15. For example, its energy parameters (like depth of the potential well and the potential barrier) better agree with the experimental values. In addition, the profile of

new surface has greater slope in the Franck–Condon region and its minimum is rather in the C_s symmetry than in the C_{2v} one. Three-dimensional quantum mechanical calculations of the bands made using the new surface¹³⁸ showed a good agreement with the experiment^{45,46} (good coincidence of spectral positions of the bands). At the same time sensitivity of calculational results to the shape of the surfaces revealed in this study makes the final identification of the transition too problematic until necessary quality of the surfaces is achieved and they themselves are thoroughly studied.

A detailed study of Huggins bands structure has been undertaken in Refs. 46 and 134, where Huggins bands of the $^{18}\text{O}_3$ isotope are obtained and used in calculations for the first time. As shown in these papers the band at $\lambda = 351.4$ nm earlier,^{45,90,109,135} was misinterpreted as the band due to the transition $(000)'' \rightarrow (000)'$ while, in fact it is due to the transition $(000)'' \rightarrow (200)'$ (see Fig. 3). Moreover, the author of papers [46] and [134] observed two longer wave "cold" bands $((000)'' \rightarrow (110)')$ and $(000)'' \rightarrow (100)'$ more in both of the isotopes. The calculated position of the band $(000)'' \rightarrow (000)'$ ($0 \rightarrow 0$, briefly) is at $\lambda = 368.7$ nm for $^{16}\text{O}_3$ and it is shifted by 19 cm^{-1} for $^{18}\text{O}_3$. The band itself has not been observed in Refs. 46 and 134, but yet in Ref. 135 there was observed the band at $\lambda = 368.8$ nm and two bands at 355.3 and

359.6 nm which could be identified as the sought transitions $0 \rightarrow 0$, $(000)'' \rightarrow (110)'$, and $(000)'' \rightarrow (100)'$, though the authors of Ref. 135 considered them to be hot bands. As to the other features of the spectrum, Katayama^{46,134} follows the same interpretation of the progressions in Huggins bands as in Ref. 45. No identification of the symmetry of the upper electronic state of the transition yielding Huggins bands has been done in Refs. 46 and 134.

3.2. Absorption cross section. During the last 40s the absorption spectrum in Huggins bands has been very carefully measured by many researchers. A summary of measurement data obtained at nearly room temperatures is presented in Fig. 3. Temperature caused variations of the absorption cross section for some spectral intervals are shown in Fig. 4. In Table I one finds the list of publications devoted to the study of the ozone absorption spectrum since 50s. As seen from this table temperature behavior of Huggins absorption bands has been studied in Refs. 92 and 93 (310–346 nm; 180–400 K), 109 (310–370 nm; 195–333 K), 114 (310–325 nm; 300–1050 K), 117 (310–350 nm; 200–300 K), 118–120 (310–350 nm; 223 and 294 K), 125 (310–350 nm; 226–298 K), 116 (mercury lines; 195, 228, and 295 K), and in 126 (339–355 nm; 220–293 K). The curves presented in Fig. 4 *b* are typical for all of Huggins bands. The spectrum structure becomes smoother as temperature increases. No pressure dependence was noticed in all of the above cited papers (see the note in the Sec. 1 of Part 1).

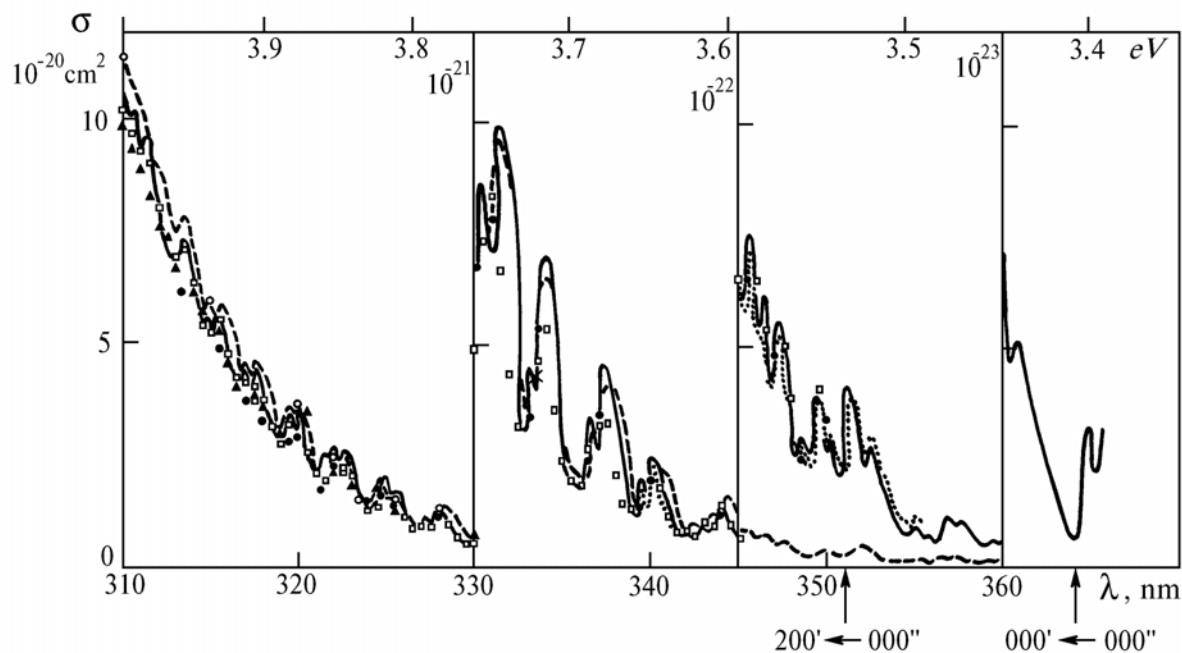


FIG. 3. Ozone absorption spectrum in Huggins bands at room temperature: 291 K, 1952/53 (Refs. 92 and 93) (by solid lines); 293 K, 1961 (Ref. 94) (by crosses); 300 K, 1973 (Ref. 109) (by dashed lines); 298 K, 1975 (Ref. 110) (by triangles); 293 K, 1982 (Ref. 114) (by open circles); 294 K, 1984 (Ref. 120) (by filled circles); 298 K, 1986 (Ref. 125) (by \square); and, 293 K, 1989 (Ref. 126) (by dots).

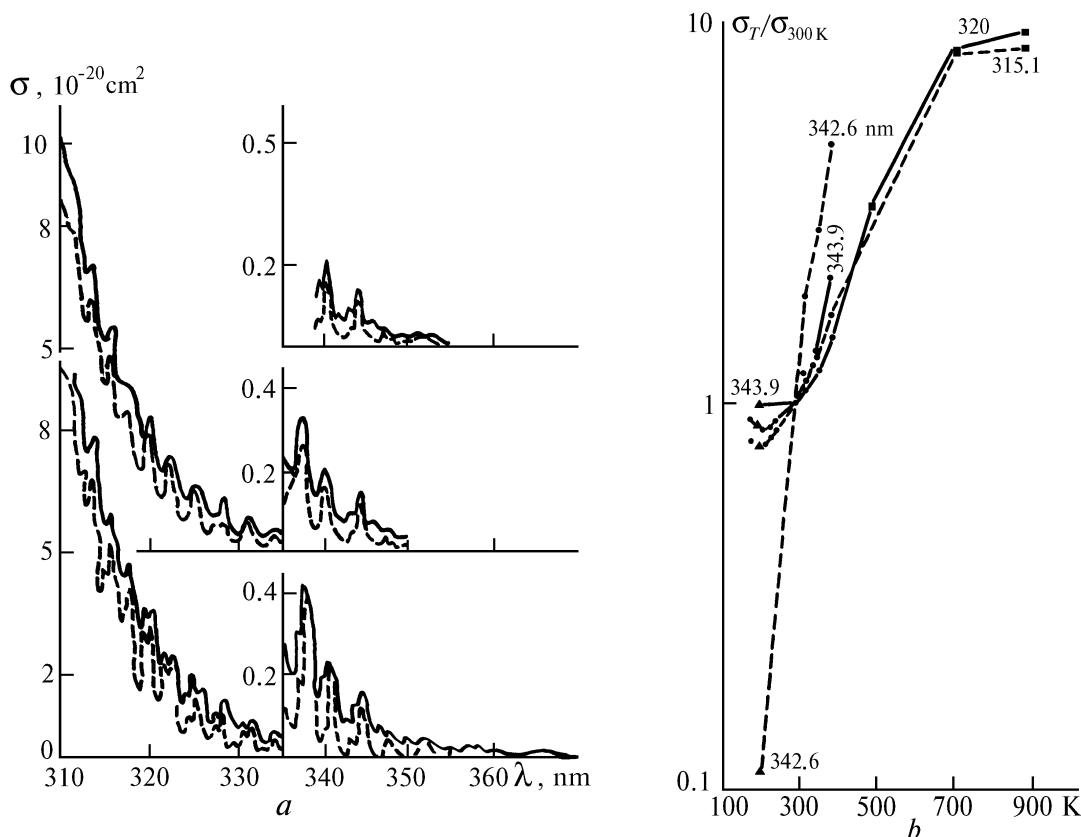


FIG. 4. The temperature influence on the absorption cross section in Huggins bands. (a) data from Ref. 109: 300 (solid line) and 195 (dashed line) (bottom plot), from Ref. 125: 298 (solid line) and 226 (dashed line) (intermediate), from Ref. 126: 293 (solid line) and 220 (dashed line) (top). (b) the change of absorption at some maxima and minima of the spectrum. The circles at some wavelengths are connected using straight lines: solid line is for maxima and dashed line is for minima.

3.3. Analysis of the photolysis products. Although the absorption within Huggins bands provides for dissociation into excited fragments, if only energy considerations are taken into account, corresponding dissociation channels are spin forbidden (see Table I in Part 1) and no excited products of dissociation have been observed in the experiments, except for the case of absorption in the region near the bands boundary at 310 nm. The latter case will be considered in our further analysis of Hartley absorption band. Energy states of the predissociation products produced due to the absorption in Huggins bands have not been studied.

3.4. Conclusions. Thus, it can be stated based on the studies discussed above that Huggins absorption bands extending from 310 to 400 nm originate due to either weak dipole-forbidden ($f \approx 10^{-4}$) electronic transition, $X^1A_1 \rightarrow 2^1A_1$ (the latter state correlates, in the diabatic approach, with a ring-shaped ozone molecule) or nonvertical transition to 1^1B_2 state (to its weakly bound local minimum of 0.6 eV). The band $0 \rightarrow 0$ is approximately at $\lambda = 368.7$ nm. The spectrum itself is purely vibrational, diffuse (because of intersection with a repulsive state⁸³ somewhere about 4 eV) and strongly depends on the temperature, especially in the regions of extrema.

The bands, in their structure, are progressions mostly over the mode ν_1' of the upper energy state with only one or two quanta from ν_2' and ν_3' modes (according to calculations

made in Refs. 45, 46, and 109, $\nu_{1,3}' = 350\text{--}370 \text{ cm}^{-1}$), the latter ones becoming irregular near the short-wave boundary (310 nm) of the band, where (at $\lambda < 313.5$ nm) Huggins and Hartley bands overlap (interaction between the electronic states 2^1A_1 and 1^1B_2 takes place). Predissociation of the ozone molecules due to absorption in Huggins bands (except for a narrow region near the boundary at 310 nm) yields the unexcited products $\text{O}(\text{}^3P) + \text{O}_2(\text{}^3\Sigma_g^-)$. The decay of the ozone molecule occurs during a short time interval covering only several periods of vibrations in the upper electronic state ($\tau_{\text{diss}} = 3.6$ fs).⁴⁸ No pressure dependence of spectra in Huggins bands have been revealed in the temperature and pressure ranges under study. It was impossible to study the bands at $\lambda < 310$ nm because of masking by the stronger Hartley absorption band.

REFERENCES

1. Ch.F. Schönbein and Lettre de M. Schönbein a M. Arago, *Compt. Rendus.* **10**, No. 17, 706 (1840).
2. W.N. Hartley, *J. Chem. Soc.* **39**, 57 (1881).
3. J. Chappuis, *Compt. Rendus* **94**, No. 15, 858 (1882).
4. W. Huggins and Mrs. Huggins, *Proc. Roy. Soc. Ser. A.* **48**, 216 (1890).
5. D.R. Salahub, S.H. Lamson, and R.F. Messmer, *Chem. Phys. Lett.* **85**, No. 4, 430 (1982).

6. V.R. Saunders and J.H. von Lenthe, *Mol. Phys.* **48**, No. 5, 923 (1983).
7. P.J. Hay, T.H. Dunning, and Jr, W.A. Goddard III, *J. Chem. Phys.* **62**, No. 10, 3912 (1975).
8. K.-H. Thunemann, S.D. Peyerimhoff, and R.J. Buenker, *J. Mol. Spectr.* **70**, No. 3, 432 (1978).
9. W.D. Laidig and H.F. Schaefer III, *J. Chem. Phys.* **74**, No. 6, 3411 (1981).
10. F. Moscardo, R. Andarias, and E. San-Fabian, *Int. J. Quant. Chem.* **34**, No. 4, 375 (1988).
11. R.D. Harcourt, F.L. Skrezenek, R.M. Wilson, and R.H. Flegg, *J. Chem. Soc. Far. Trans. II* **82**, No. 4, 495 (1986).
12. K.A. Peterson, R.C. Mayrhofer, E.L. Sibert III, and R.C. Woods, *J. Chem. Phys.* **94**, No. 1, 414 (1991).
13. K.V. Ermakov, B.S. Butaev, and V.P. Spiridonov, *J. Mol. Struct.* **240**, 295 (1990).
14. J.S. Wright, S.-K. Shih, and R.J. Buenker, *Chem. Phys. Lett.* **75**, No. 3, 513 (1980).
15. M.G. Sheppard and R.B. Walker, *J. Chem. Phys.* **78**, No. 12, 7191 (1983).
16. S. Carters, I.M. Mills, J.N. Murrell, and A.J.C. Varandas, *Mol. Phys.* **45**, No. 5, 1053 (1982).
17. J.M. Standard and M.E. Kellman, *J. Chem. Phys.* **94**, No. 7, 4714 (1991).
18. A.D. Walsh, *J. Chem. Soc.* **3**, No. 8, 2266 (1953).
19. R.S. Mulliken, *Can. J. Chem.* **36**, No. 1, 10 (1958).
20. S.D. Peyerimhoff and R.J. Buenker, *J. Chem. Phys.* **47**, No. 6, 1953 (1967).
21. R.J. Celotta, S.R. Mielczarek, and C.E. Kuyatt, *Chem. Phys. Lett.* **24**, No. 3, 428 (1974).
22. P.J. Hay and T.H. Dunning, Jr., *J. Chem. Phys.* **67**, No. 5, 2290 (1977).
23. C.R. Brundle, *Chem. Phys. Lett.* **26**, No. 1, 25 (1974).
24. D.C. Frost, S.T. Lee, and C.A. McDowell, *Chem. Phys. Lett.* **24**, No. 2, 149 (1974).
25. S. Trajmar, J.K. Rice, and A. Kuppermann, *Adv. Chem. Phys.* **18**, 15 (1970).
26. M. Inokuti, *Rev. Mod. Phys.* **43**, No. 3, 297 (1971).
27. D. Grimbert and A. Devaquet, *Mol. Phys.* **27**, No. 4, 831 (1974).
28. S. Shih, R.J. Buenker, and S.D. Peyerimhoff, *Chem. Phys. Lett.* **28**, No. 4, 463 (1974).
29. L.B. Harding and W.A. Goddard III, *J. Chem. Phys.* **67**, No. 5, 2377 (1977).
30. M.J.S. Dewar, S. Olivella, and H.S. Rzepa, *Chem. Phys. Lett.* **47**, No. 1, 80 (1977).
31. R.R. Lucchese and H.F. Schaefer, *J. Chem. Phys.* **67**, No. 2, 848 (1977).
32. G. Karlström, S. Engström, and B. Jonsson, *Chem. Phys. Lett.* **57**, No. 3, 390 (1978).
33. P.G. Burton, *Int. J. Quant. Chem.* No. 11, 207 (1977).
34. P.G. Burton, *J. Chem. Phys.* **71**, No. 2, 961 (1979).
35. C.W. Wilson and Jr, D.G. Hopper, *J. Chem. Phys.* **74**, No. 1, 595 (1981).
36. R.O. Jones, *Phys. Rev. Lett.* **52**, No. 22, 2002 (1984).
37. R.O. Jones, *J. Chem. Phys.* **82**, No. 1, 325 (1985).
38. M. Morin, A.E. Foti, and D.R. Salahub, *Can. J. Chem.* **63**, No. 7, 1982 (1985).
39. W.G. Laidlaw and M. Trisic, *Can. J. Chem.* **63**, No. 7, 2044 (1985).
40. T.J. Lee, *Chem. Phys. Lett.* **169**, No. 6, 529 (1990).
41. A. Banichevich, S.D. Peyerimhoff, and F. Green, *Chem. Phys. Lett.* **173**, No. 1, 1 (1990).
42. S.S. Xantheas, G.J. Atchity, S.T. Elbert, and K. Ruedenberg, *J. Chem. Phys.* **94**, No. 12, part. 1, 8054 (1991).
43. J.F. Riley and R.W. Cahill, *J. Chem. Phys.* **52**, 3297 (1970).
44. C.W. Von Rosenberg and Jr, D.W. Trainor, *J. Chem. Phys.* **61**, No. 6, 2442 (1974), *ibid.* **63**, No. 12, 5348 (1975).
45. J.C.D. Brand, K.J. Cross, and A.R. Hoy, *Can. J. Phys.* **56**, 327 (1978).
46. D.H. Katayama, *J. Chem. Phys.* **71**, No. 2, 815 (1979).
47. J.F. Hiller and M.L. Vestal, *J. Chem. Phys.* **77**, No. 3, 1248 (1982).
48. A. Sinha, D. Imre, J.H. Goble, Jr, and J.L. Kinsey, *J. Chem. Phys.* **84**, No. 11, 6108 (1986).
49. S.M. Anderson, J. Morton, and K. Mauersberger, *J. Chem. Phys.* **93**, No. 6, 3826 (1990).
50. S.M. Anderson, J. Maeder, and K. Mauersberger, *J. Chem. Phys.* **94**, No. 10, 6351 (1991).
51. A.A. Turnipseed, G.L. Vaghjiani, T. Gierczak et. al., *J. Chem. Phys.* **95**, No. 5, 3244 (1991).
52. D.R. Stull, H. Prophet et. al., NSRDS-NBS 37, Office of Standard Reference Data, National Bureau of Standards, Washington, DC, Contract No. F04611-67-C-0009 (1971).
53. J.L. Gole and R.N. Zare, *J. Chem. Phys.* **57**, 5331 (1972).
54. M.J. Weiss, J. Berkowitz, and E.H. Appelman, *J. Chem. Phys.* **66**, No. 5, 2049 (1977).
55. R. Krishna and K.D. Jordan, *Chem. Phys.* **115**, No. 3, 423 (1987).
56. R.H. Hughes, *J. Chem. Phys.* **24**, No. 1, 131 (1956).
57. T. Tanaka and Y. Morino, *J. Mol. Spectr.* **33**, No. 3, 538 (1970).
58. S.S. Xantheas, S.T. Elbert, and K. Ruedenberg, *J. Chem. Phys.* **93**, No. 10, 7519 (1990).
59. L.L. Lohr and A.J. Helman, *J. Chem. Phys.* **86**, No. 10, 5329 (1987).
60. A. Devaquet and J. Ryan, *Chem. Phys. Lett.* **22**, No. 2, 269 (1973).
61. S.E. Frish, *Optical Spectra of Atoms*. Chapter VII (Fiz. Mat. Literature Press, Moscow, 1963).
62. M.J. Kurylo, W. Braun, and A. Kaldor, *Chem. Phys. Lett.* **27**, 249 (1974).
63. J.I. Steinfeld, S.M. Adler-Golden, and J.W. Gallagher, *J. Phys. Chem. Ref. Data* **16**, No. 4, 911 (1987).
64. C. Flannery, J.J. Klaassen, M. Gojer et. al., *J. Quant. Spectr. Rad. Trans.* **46**, No. 2, 73 (1991).
65. M.N. Spenser and G. Chackerian, Jr, *J. Mol. Spectr.* **146**, No. 1, 135 (1991).
66. V. Vaida, D.J. Donaldson, S.J. Strickler, et. al., *J. Phys. Chem.* **93**, No. 2, 506 (1989).
67. A.J. Sedlacek and C.A. Wight, *J. Phys. Chem.* **93**, No. 2, 509 (1989).
68. N. Swanson and R.J. Celotta, *Phys. Rev. Lett.* **35**, No. 12, 783 (1975).
69. R.J. Celotta, N. Swanson, and M. Kurepa, *Proc. of Xth IPEAC Conference*, July (1977).
70. O.P. Wulf, *Proc. Nat. Acad. Sci.* **16**, No. 7, 507 (1930).
71. P.J. Hay and W.A. Goddard III, *Chem. Phys. Lett.* **14**, No. 1, 46 (1972).
72. P.J. Hay, T.H. Dunning, Jr, and W.A. Goddard III, *Chem. Phys. Lett.* **23**, No. 4, 457 (1973).
73. G. Herzberg, *Molecular Spectra and Molecular Structure*, Vol. 2, *Infrared and Raman Spectra of Polyatomic Molecules* (Van Nostrand, New York, 1945).

74. L. Lefebvre, C.R. Acad. Sci. (Paris) **200**, No. 21, 1743 (1935).
75. R.P. Messmer and D.R. Salahub, J. Chem. Phys. **65**, No. 2, 779 (1976).
76. W.D. McGrath, A. Thompson, and J. Trocha-Grimshaw, Plan. Space Sci. **34**, No. 11, 1147 (1986).
77. S.E. Novick, P.C. Engelking, P.L. Jones et al., J. Chem. Phys. **70**, No. 6, 2652 (1979).
78. J.F. Hiller and M.L. Vestal, J. Chem. Phys. **74**, No. 1, 6096, 1981.
79. S. Kuis, R. Simonaitis, and J. Heicklen, J. Geoph. Res. **80**, 28 (1975).
80. J. Shi and J.R. Barker, J. Phys. Chem. **94**, No. 22, 8390 (1990).
81. J.S. Wright, Can. J. Chem. **51**, No. 1, 139 (1973).
82. W.G. Laidlaw and M. Trisic, Chem. Phys. **36**, 323 (1979).
83. P.J. Hay, R.T. Pack, R.B. Walker, and E.J. Heller, J. Phys. Chem. **86**, No. 6, 862 (1982).
84. A.J.C. Varandas and A.A.C.C. Pais, Mol. Phys. **65**, No. 4, 846 (1988).
85. M. Griggs, J. Chem. Phys. **49**, No. 2, 857 (1968).
86. M. Lichtenstein, J.J. Gallagher, and S.A. Clough, J. Mol. Spectr. **40**, 10 (1971).
87. E.C.Y. Inn and Y. Tanaka, J. Opt. Soc. Am. **43**, No. 10, 870 (1953).
88. Y. Tanaka, E.C.Y. Inn, and K. Watanabe, J. Chem. Phys. **21**, No. 10, 1651 (1953).
89. L.A. Curtiss, S.R. Langhoff, and G.D. Carney, J. Chem. Phys. **71**, No. 12, 5016 (1979).
90. C.-W. Lui and B.T. Darling, J. Mol. Spectr. **21**, No. 2, 146 (1966).
91. E.C.Y. Inn and Y. Tanaka, *Ozone Absorption Coefficients in Visible and Ultraviolet Region. In: Ozone Chemistry and Technology*. Wash., 263–268 (1959).
92. E. Vigroux, Compt. Rend. Acad. Sci. (Paris), **234**, No. 24, 2351; No. 25, 2439; No. 26, 2529; N 27, 2592 (1952).
93. E. Vigroux, Annal. Phys. **8**, 709 (1953).
94. A.G. Hearn, Proc. Phys. Soc., Ser. A. **78**, No. 504, 932 (1961).
95. A.M. Bass and R.J. Paur, J. Photoch. **17**, No. 1/2, 141 (1981).
96. A. Amoroso, M. Cacciani, A. di Sarra, and G. Fiocco, J. Geoph. Res. **95**, No. D12, 20565 (1990).
97. C.E. Fairchild, E.J. Stone, and G.M. Lawrence, J. Chem. Phys. **69**, No. 8, 3632 (1978).
98. J.J. Valentini, D.S. Moore, and D.S. Bomse, Chem. Phys. Lett. **83**, No. 2, 217 (1981).
99. D.S. Moore, D.S. Bomse, and J.J. Valentini, J. Chem. Phys. **79**, No. 4, 1745 (1983).
100. H.B. Levene, J.-C. Nieh, and J.J. Valentini, J. Chem. Phys. **87**, No. 5, 2583 (1987).
101. W.D. McGrath, J.M. Maguire, A. Tompson, and J. Trocha-Grimshaw, Chem. Phys. Lett. **102**, No. 1, 59 (1983).
102. I.C. McDade, and W.D. McGrath, Chem. Phys. Lett. **72**, No. 3, 432 (1980).
103. I.C. McDade and W.D. McGrath, Chem. Phys. Lett. **73**, No. 3, 413 (1980).
104. S.M. Adler-Golden, E.L. Schweitzer, and J.I. Steinfeld, J. Chem. Phys. **76**, No. 5, 2201 (1982).
105. K. Watanabe, Adv. in Geophys. **5**, 153 (1956).
106. M. Ogawa and C.R. Cook, J. Chem. Phys. **28**, No. 1, 173 (1958).
107. W.M. Jones and N. Davidson, J. Am. Chem. Soc. **84**, No. 15, 2868 (1962).
108. W.B. DeMore and O.F. Raper, J. Phys. Chem. **68**, No. 2, 412 (1964).
109. J.W. Simons, R.J. Paur, and H.A. Webster III, J. Chem. Phys. **59**, No. 2, 1203 (1973).
110. G.K. Moortgat and P. Warneck, Z. Naturforsch. **30a**, 835 (1975).
111. J.A. Hanvey and W.D. McGrath, Chem. Phys. Lett. **36**, No. 5, 564 (1975).
112. I. Arnold, F.J. Comes, and G.K. Moortgat, Chem. Phys. **24**, 211 (1977).
113. P.W. Fairchild and E.K.C. Lee, Chem. Phys. Lett. **60**, No. 1, 36 (1978).
114. D.D. Astholz, A.E. Crose, and J. Troe, J. Phys. Chem. **86**, No. 5, 696 (1982).
115. D.E. Freeman, K. Yoshino, L.T. Esmond, and W.H. Parkinson, Plan. Space Sci. **32**, No. 2, 239 (1984).
116. K. Yoshino, D.E. Freeman, J.R. Esmond, and W.H. Parkinson, Plan. Space Sci. **36**, No. 4, 396 (1988).
117. A.M. Bass and R.J. Paur, *Proceedings of the Quadrennial Intern. Ozone Symp.* ed. by J. London (NCAR, Boulder, CO, 1981), **1**, 140–145; in: *Proceedings of the Quadrennial Ozone Symp.* (Halkidiki, Greece, 3–7 Sept. 1984), ed. by C.S. Zerefos and A. Ghazi (D. Reidel, Dordrecht, Holland, 1985), 606–616.
118. D. Daumont, J. Brion, and J. Malicet, Plan. Space Sci. **31**, 1229 (1983).
119. J. Malicet, J. Brion, and D. Daumont, in: *Atmospheric Ozone, Proceedings of the Quadrennial Ozone Symp.* (Halkidiki, Greece, 3–7 Sept. 1984) ed. by C.S. Zerefos and A. Ghazi (D. Reidel, Dordrecht, Holland, 1985), 617–621.
120. J. Brion, D. Daumont, and J. Malicet, J. de Phys. Lett. (Paris), **45**, No. 2, L57 (1984).
121. J. Brion, D. Daumont, J. Malicet, and P. Marche, J. de Phys. Lett. (Paris), **46**, No. 3, L105 (1985).
122. K. Mauersberger, J. Barnes, D. Hanson, and J. Morton, Geophys. Res. Lett. **13**, No. 7, 671 (1986).
123. K. Mauersberger, D. Hanson, J. Barnes, and J. Morton, J. Geophys. Res. **92**, No. D7, 8480 (1987).
124. J. Barnes and K. Mauersberger, J. Geophys. Res. **92**, No. D12, 14861 (1987).
125. L.T. Molina and M.J. Molina, J. Geophys. Res. **91**, No. D13, 14501 (1986).
126. M. Cacciani, A. di Sarra, G. Fiocco, and A. Amoroso, J. Geophys. Res. **94**, No. D6, 8485 (1989).
127. S.N. Tkachenko, V.E. Zhuravlev, M.P. Popovich et al., Zh. Fiz. Khim. **54**, No. 9, 2289 (1980).
128. H.B. Levene and J.J. Valentini, J. Chem. Phys. **87**, No. 5, 2594 (1987).
129. J.J. Valentini, Chem. Phys. Lett. **96**, No. 4, 395 (1983).
130. J.J. Valentini, D.P. Gerrity, D.L. Phillips, et al., J. Chem. Phys. **86**, No. 12, 6745 (1987).
131. A. Jakowlewa and V. Kondratjev, Phys. Z. der Sowjet **1**, No. 4, 471 (1932); **9**, No. 1, 106 (1936).
132. B.R. Jonson and J.L. Kinsey, J. Chem. Phys. **91**, No. 12, 7638 (1989).
133. D. Chalonge and L. Lefebvre, C.R. Hebd. Seances Acad. Sci. **197**, 444 (1933).
134. D.H. Katayama, J. Chem. Phys. **85**, No. 11, 6809 (1986).
135. W.H. Eberhardt and W. Shand, J. Chem. Phys. **14**, 525 (1946).
136. A. Banichevich, S.D. Peyerimhoff, J.A. Beswick, and O. Atabek, J. Chem. Phys. **96**, 6580 (1992).
137. K. Yamashita, K. Morokuma, F. Le Quere, and C. Leforestier, Chem. Phys. Lett. **191**, No. 6, 515 (1992).
138. F. Le Quere and C. Leforestier, Chem. Phys. Lett. **189**, No. 6, 537 (1992).